Spectrochimica Acta Part A: Molecular and Biomolecular Spectroscopy 110 (2013) 20–27

Contents lists available at SciVerse ScienceDirect

Spectrochimica Acta Part A: Molecular and Biomolecular Spectroscopy

journal homepage: www.elsevier.com/locate/saa

Synthesis and evaluation of gold(III) complexes as efficient DNA binders and cytotoxic agents

Mohan N. Patel *, Bhupesh S. Bhatt, Promise A. Dosi

Department of Chemistry, Sardar Patel University, Vallabh Vidyanagar, 388 120 Gujarat, India

HIGHLIGHTS

- Synthesis and characterization of gold(III) complexes.
- DNA interactions studies suggest complexes as covalent binder.
- Brine shrimp lethality bioassay was performed to check the cytotoxicity of complexes.
- Michaelis–Menten kinetic calculations for DNA cleavage reaction.

GRAPHICAL ABSTRACT

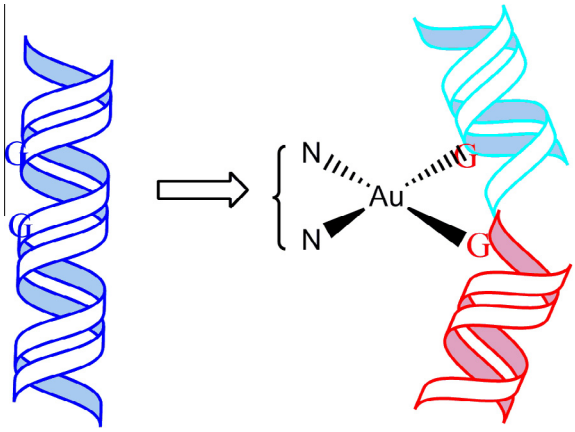

ARTICLE INFO

Article history:
Received 17 December 2012
Received in revised form 23 February 2013
Accepted 3 March 2013
Available online 14 March 2013

Keywords:
Au(III) complex
Michaelis–Menten kinetic
Covalent binding
Rate constant

ABSTRACT

In recent years, great interest has been focused on gold(III) complexes as cytotoxic and antitumor drugs. Recent studies demonstrated that simple bidentate or polydentate ligands containing nitrogen donor atoms may offer sufficient redox stabilization to produce viable Au(III) anticancer drug targets under physiologic conditions. So, we have synthesized square planer Au(III) complexes of type $[Au(A^n)Cl_x]\cdot Cl_y$ and characterized them using UV–Vis absorption, C, H, N elemental analysis, FT-IR, LC–MS, ^1H and ^{13}C NMR spectroscopy. These compounds manifested significant cytotoxic properties *in vitro* for brine shrimp lethality bioassay. The metal complexes were screened for series of DNA binding activity using UV–Vis absorption titration, hydrodynamic measurement and thermal DNA denaturation study. The nucleolytic activity was performed on plasmid pUC19 DNA. The Michaelis–Menten kinetic studies were performed to evaluate rate of enhancement in metal complexes mediated DNA cleavage over the non-catalyzed DNA cleavage.

Introduction

Interaction between DNA and drug molecules is of current general interest and importance [1,2], especially for the designing of new DNA-targeted drugs and the screening of these *in vitro*. Research into the reactivity and interactions between transition metal complexes and biomolecules such as DNA and proteins has resulted in significant advances in the understanding of biochemical processes and the development of therapeutic drugs. Since it was found that cancer could be treated with *cis*-$[Pt(NH_3)_2Cl_2]$ [3], interest has been activized to explore the anti-cancer activity of metal complexes [4,5]. Study on the interactions of metal complexes with nucleic acids is just one of the basic

* Corresponding author. Tel.: +91 2692 226856x218.
E-mail address: jeenen@gmail.com (M.N. Patel).

1386-1425/$ - see front matter © 2013 Elsevier B.V. All rights reserved.
http://dx.doi.org/10.1016/j.saa.2013.03.037

researches to catch on the biological effect of complexes on nucleic acids and select potential anti-cancer active medicines [6]. Many metal-derived drugs [7] are believed to inhibit DNA synthesis in rapidly growing cells, such as cancer cells, by binding to their DNA. The formation of these adducts alters DNA structure in such a way that replication either cannot proceed or results in nonviable daughter cells [8,9]. Thus, advances in the design and synthesis of new anticancer agents require exhaustive knowledge of the different DNA-binding mechanisms with a view to obtaining other more selective agents. There are many methods to study the DNA binding properties [3–6]. One of the routine, very common and convincing procedures used to study the interactions of different compounds with DNA is spectrophotometric measurements [6].

There are many reports on organic metal complexes that are capable of binding to DNA [10]. The organic metal complexes have some advantages, such as easy preparation and variety of design possibilities with different metal ions and ligands, for probing DNA structure and investigating the binding process as well as for facilitating individual applications. Among them, ruthenium complex is one of the most extensively investigated members of a class of the DNA-binding organic metal complexes. However, only little attention has been paid to the other metal complexes as DNA interacting agent. Among them, Au(III) compounds, isoelectronic and isostructural with Pt(II) compounds, are emerging as efficient DNA binders and anticancer agents [11–13]. Therefore, to elucidate biochemical aspects of gold(III) compounds under physiological conditions and, specifically, the reactivity of gold(III) compounds with DNA, in continuation of our earlier work [14], we have synthesized Au(III) complexes of 2,2′-(phenylmethylene)bis(1H-pyrrole) (A^1)/2,2′-((4-chlorophenyl)methylene) bis(1H-pyrrole) (A^2)/N^2,N^6-bis(pyridin-2-yl)pyridine-2,6-dicarboxamide (A^3)/N-(pyridin-2-yl) picolinamide (A^4)/4-chloro-N-(pyridin-2-ylmethyl)aniline (A^5) and characterized them using different analytical and spectroscopic techniques. The compounds were checked for different DNA interaction, kinetic and cytotoxic studies.

Experimental

Materials

All the chemicals and solvents were of reagent grade and used as purchased. Chloroauric acid, 4-chloroaniline, 2-aminopyridine, TFA and sodium borohydride were purchased from S.d. fine-chem Ltd. (India.). EDTA, pyrrole, benzaldehyde and *p*-chloro benzaldehyde were purchased from Spectrochem Pvt. Ltd. (India). 2-Picolinic acid and 2,6-dipicolinic acid was purchased from Alfa Aesar (England). Ethidium bromide was purchased from Himedia (India). Herring Sperm DNA was purchased from Sigma Chemical Co. (India).

Instrumentation

Infrared spectra were recorded on ABB Bomen MB 3000, FT–IR spectrophotometer as KBr pellets in the range 4000–400 cm^{-1}. The LC–MS were recorded using Thermo Scientific mass spectrophotometer (USA). The ^1H NMR and ^{13}C NMR were recorded on a Bruker Advance (400 MHz, Germany). The electronic spectra were recorded on a TCC-240 A, UV–Vis spectrophotometer, Shimadzu (Japan). Thermal DNA denaturation study was performed using Agilent 8453 UV–Vis spectrophotometer. C, H and N elemental analyses were performed with a model 240 Perkin Elmer elemental analyzer.

Synthesis of ligands

2,2′-(Phenylmethylene)bis(1H-pyrrole) (A^1)

2,2′-(Phenylmethylene)bis(1H-pyrrole) was prepared via condensation of the benzaldehyde and pyrrole under TFA catalysis [15,16]. Yield: 29%, m.p.: 128 °C, Anal. Calc. for $C_{15}H_{14}N_2$ (222.29): C, 81.05; H, 6.35; N, 12.60%. Found: C, 81.24; H, 6.52; N, 12.47%. ^1H NMR (DMSO-d_6, 400 MHz): δ (ppm) 7.39 (d, 2H, $H_{3'',5''}$, $J = 8$), 7.28 (d, 2H, $H_{2'',6''}$, $J = 8$), 7.18 (t, 1H, $H_{4''}$, $J = 6.8$), 6.37–6.36 (complex, 2H, $H_{5,5'}$), 5.94 (t, 2H, $H_{4,4'}$, $J = 7.2$), 5.77 (d, 2H, $H_{3,3'}$, $J = 8$), 5.27 (s, 2H, —NH), 5.15 (s, 1H, —CH). ^{13}C NMR (DMSO-d_6, 100 MHz): δ (ppm) 146.07. ($C_{1''}$), 139.35 ($C_{2,2'}$), 137.92 ($C_{2'',6''}$), 136.48 ($C_{3'',5''}$), 133.80 ($C_{4''}$), 126.36 ($C_{5,5'}$), 114.57 ($C_{4,4'}$), 112.49 ($C_{3,3'}$), 48.19 (C_{CH}). FT-IR (cm^{-1}): 3420 (m), 3060 (w), 1590 (s), 1530 (s), 1380 (s), 1120 (w), 760 (s), 720 (m), 660 (m).

2,2′-((4-Chlorophenyl)methylene)bis(1H-pyrrole) (A^2)

2,2′-((4 Chlorophenyl)methylene)bis(1H-pyrrole) was prepared via condensation of the *p*-chlorobenzaldehyde and pyrrole under TFA catalysis [15,16]. Yield: 26%, m.p.: 135 °C, Anal. Calc. for $C_{15}H_{13}ClN_2$ (256.73): C, 70.18; H, 5.10; N, 10.91%. Found: C, 70.35; H, 5.23; N, 11.02%. ^1H NMR (DMSO-d_6, 400 MHz): δ (ppm) 7.43 (d, 2H, $H_{3'',5''}$, $J = 8$), 7.28 (d, 2H, $H_{2'',6''}$, $J = 8$), 6.36–6.36 (complex, 2H, $H_{5,5'}$), 5.93 (t, 2H, $H_{4,4'}$, $J = 7.2$), 5.77 (d, 2H, $H_{3,3'}$, $J = 8$), 5.26 (s, 2H, —NH), 5.14 (s, 1H, —CH). ^{13}C NMR (DMSO-d_6, 100 MHz): δ (ppm) 145.53 ($C_{1''}$), 144.82 ($C_{4''}$), 141.16 ($C_{2,2'}$), 139.33 ($C_{2'',6''}$), 138.09 ($C_{3'',5''}$), 127.41 ($C_{5,5'}$), 114.67 ($C_{4,4'}$), 112.93 ($C_{3,3'}$), 48.26 (C_{CH}). FT-IR (cm^{-1}): 3430 (m), 3080 (w), 1600 (s), 1530 (s), 1390 (s), 1120 (s), 1060 (s), 770 (s), 720 (s), 660 (m).

N^2,N^6-bis(pyridin-2-yl)pyridine-2,6-dicarboxamide (A^3)

A mixture of dipicolinic acid (10 mmol) and thionylchloride (20 mL) were refluxed for 4–5 h, till the evolution of HCl gas ceases, under anhydrous condition. Excess thionylchloride was removed under reduced pressure. The resulting solution was cooled in an ice bath for 15 min. Dry toluene (25–30 mL) followed by 2-aminopyridine (20 mmol) was added to the above solution and further refluxed until no more HCl was evolved. The solvent was removed under reduced pressure and the resultant white solid was washed with petroleum ether and neutralized with 5% $NaHCO_3$. It was filtered, washed with water and then alcohol. Recrystallization from chloroform and ethanol yield silky needles and air-dried. Yield: 88%, m.p.: 219 °C, Anal. Calc. for $C_{17}H_{13}N_5O_2$ (319.32): C, 63.94; H, 4.10; N, 21.93. Found: C, 63.80; H, 4.22; N, 21.78%. ^1H NMR ($CDCl_3$-*d*, 400 MHz): δ (ppm) 11.26 (s, 2H, —NH), 8.56–8.52 (complex, 4H, $H_{3,5,6',6''}$), 8.40 (dd, 2H, $H_{3',3''}$, $J = 0.8$, $J = 4.8$), 8.17 (t, 1H, H_4, $J = 8$), 7.83 (dt, 2H, $H_{4',4''}$, $J = 1.6$, $J = 8$), 7.14 (t, 2H, $H_{5',5''}$, $J = 6$). ^{13}C NMR ($CDCl_3$-*d*, 100 MHz): δ (ppm) 164.92 (C_{CO}), 150.40 ($C_{2',2''}$), 149.78 ($C_{2,6}$), 148.55 ($C_{6',6''}$), 142.47 (C_4), 140.35 ($C_{4',4''}$), 126.92 ($C_{3,5}$), 120.06 ($C_{5',5''}$), 115.21 ($C_{3',3''}$). FT-IR (cm^{-1}): 3390 (w), 3050 (m), 1700 (s), 1580 (s), 1530 (s), 1440 (s), 1320 (s), 1240 (w), 1150 (m), 780 (m), 670 (m).

N-(Pyridin-2-yl)picolinamide (A^4)

It was prepared following the same procedure above by taking 2-picolinic acid as starting reactant. Yield: 83%, m.p.: 163 °C, Anal. Calc. for $C_{11}H_9N_3O$ (199.21): C, 66.32; H, 4.55; N, 21.09. Found: C, 66.56; H, 4.74; N, 21.20%. ^1H NMR ($CDCl_3$-*d*, 400 MHz): δ (ppm) 10.45 (s, 1H, —NH), 8.56 (d, 1H, H_6, $J = 5.2$), 8.45 (d, 1H, H_3, $J = 5.2$), 8.40 (t, 1H, H_4, $J = 4.4$), 8.32 (d, 1H, $H_{6'}$, $J = 6.4$), 7.93 (t, 1H, H_5, $J = 7.6$), 7.79 (t, 1H, $H_{4'}$, $J = 8$), 7.51 (dt, 1H, $H_{5'}$, $J = 1.6$, $J = 4.8$), 7.11 (dd, 1H, $H_{3'}$, $J = 6.4$, $J = 12$). ^{13}C NMR ($CDCl_3$-*d*, 100 MHz): δ (ppm) 160.75 (C_{CO}), 150.38 ($C_{2'}$), 149.78 ($C_{2,6}$), 148.55 ($C_{6',6''}$), 148.24 (C_6), 143.48 ($C_{4'}$), 140.01 (C_4), 130.59 (C_5), 128.53 (C_3), 118.25 ($C_{5'}$), 115.68 ($C_{3'}$). FT-IR (cm^{-1}): 3350 (m),

3060 (w), 1690 (s), 1580 (s), 1520 (s), 1440 (s), 1300 (s), 1220 (m), 1150 (m), 780 (s), 690 (s).

4-Chloro-N-(pyridin-2-ylmethyl)aniline (A^5)

4-Chloroaniline (14.8 mmol) and pyridine-2-carbaldehyde (7.40 mmol) were dissolved in 50 mL of absolute ethanol to give a brownish-yellow solution, which was stirred for 1 h. Sodium borohydride in 10-fold excess (37.0 mmol) was added in portions to the ethanolic solution at 0 °C, and stirring was continued for 20 min. The solution was then refluxed for 30 min. After cooling of the yellow solution, the ethanol was removed by rotary evaporation. Water (200 mL) was added to give a yellow solution with some precipitate present. Concentrated HCl (ca. 2 mL) was added to neutralize the solution (pH ca. 6–7), causing the color of the solution to lighten and giving an off-white precipitate. The solid mass was collected and dried. Yield: 81%, m.p.: 136 °C, Anal. Calc. for $C_{12}H_{11}ClN_2$ (218.68): C, 65.91; H, 5.07; N, 12.81. Found: C, 65.83; H, 4.89; N, 12.94%. ^{1}H NMR ($CDCl_3$-*d*, 400 MHz): δ (ppm) 8.60 (d, 1H, H_6, J = 4.8), 7.67 (tt, 1H, H_4, J = 1.6, J = 7.6), 7.33 (d, 1H, H_3, J = 7.6), 7.22 (t, 1H, H_5, J = 6.4), 7.138 (ddd, 2H, $H_{3',5'}$, J = 3.2, J = 4.0, J = 5.6), 6.61 (ddd, 2H, $H_{2',6'}$, J = 3.2, J = 4.0, J = 5.6), 4.86 (s, 1H, —NH), 4.45 (d, 2H, —CH_2, J = 5.2). ^{13}C NMR ($CDCl_3$-*d*, 100 MHz): δ (ppm) 155.26 (C_2), 148.31 (C_6), 147.58 ($C_{1'}$), 141.60 (C_4), 136.74 ($C_{3',5'}$), 130.46 ($C_{4'}$), 122.53 (C_3), 121.72 (C_5), 116.02 ($C_{2',6'}$), 47.04 (C_{CH}). FT-IR (cm^{-1}): 3330 (m), 3010 (m), 1600 (s), 1480 (s), 1440 (m), 1320 (w), 1280 (m), 1190 (s), 1140 (m), 740 (s), 650 (w).

Synthesis of Au(III) complexes

*[Au(A^1)Cl_2]·Cl (**1**)*

To a solution of $H[AuCl_4]\cdot 3H_2O$ (0.5 mmol) in absolute ethanol (20 mL) was added A^1 (0.5 mmol), resulted in an immediate formation of light orange precipitate. The reaction mixture was stirred for 2 h at 60 °C. The product was isolated by filtration, washed with ether and dried. Yield: 82%, m.p.: 226 °C, Anal. Calc. for $C_{15}H_{14}AuCl_3N_2$ (525.61): C, 34.28; H, 2.68; N, 5.33%. Found: C, 34.46; H, 2.81; N, 5.20%. Λm (1×10^{-3} mol L^{-1} in DMF): 91 mho cm^2 $mole^{-1}$. ^{1}H NMR (DMSO-d_6, 400 MHz): δ (ppm) 7.50 (d, 2H, $H_{3'',5''}$, J = 8), 7.36 (d, 2H, $H_{2'',6''}$, J = 8), 7.24 (t, 1H, $H_{4''}$, J = 6.8), 6.79–6.78 (complex, 2H, $H_{5,5'}$), 6.20 (s, 2H, —NH), 6.05 (t, 2H, $H_{4,4'}$, J = 7.2), 5.99 (d, 2H, $H_{3,3'}$, J = 8), 5.20 (s, 1H, —CH). ^{13}C NMR (DMSO-d_6, 100 MHz): δ (ppm) 151.24 ($C_{1''}$), 141.37 ($C_{3,3'}$), 136.59 ($C_{2,2'}$), 135.77 ($C_{3'',5''}$), 135.38 ($C_{2'',6''}$), 134.12 ($C_{4''}$), 130.32 ($C_{5,5'}$), 115.95 ($C_{4,4'}$), 52.67 (C_{CH}). FT-IR (cm^{-1}): 3490 (m), 3070 (w), 1630 (s), 1540 (s), 1400 (s), 1180 (w), 760 (s), 730 (m), 660 (m). UV–Vis (DMSO): 276 nm (ε = 21,342 M^{-1} cm^{-1}), 334 nm (ε = 24,573 M^{-1} cm^{-1}); (Buffer): 256 nm (ε = 17,200 M^{-1} cm^{-1}), 322 nm (ε = 12,712 M^{-1} cm^{-1}), 374 nm (ε = 2680 M^{-1} cm^{-1}). LC–MS: m/z 489.03 $[Au(A^1)Cl_2]^+$.

*[Au(A^2)Cl_2]·Cl (**2**)*

Similar procedure was followed using A^2 as ligand, resulted in yellow precipitate. Yield: 81%, m.p.: 226 °C, Anal. Calc. for $C_{15}H_{13}AuCl_4N_2$ (560.06): C, 32.17; H, 2.34; N, 5.00%. Found: C, 31.94; H, 2.51; N, 5.11%. Λm (1×10^{-3} mol L^{-1} in DMF): 89 mho cm^2 $mole^{-1}$. ^{1}H NMR (DMSO-d_6, 400 MHz): δ (ppm) 7.49 (d, 2H, $H_{3'',5''}$, J = 8), 7.37 (d, 2H, $H_{2'',6''}$, J = 8), 6.79–6.78 (complex, 2H, $H_{5,5'}$), 6.09 (s, 2H, —NH), 5.95 (t, 2H, $H_{4,4'}$, J = 7.2), 5.85 (d, 2H, $H_{3,3'}$, J = 8), 5.31 (s, 1H, —CH). ^{13}C NMR (DMSO-d_6, 100 MHz): δ (ppm) 152.33 ($C_{1''}$), 141.84 ($C_{3,3'}$), 140.66 ($C_{4''}$), 139.58 ($C_{2'',6''}$), 138.24 ($C_{2,2'}$), 136.73 ($C_{3'',5''}$), 130.95 ($C_{5,5'}$), 117.40 ($C_{4,4'}$), 52.88 (C_{CH}). FT-IR (cm^{-1}): 3490 (m), 3090 (w), 1640 (s), 1540 (s), 1400 (s), 1180 (s), 1080 (s), 790 (s), 730 (s), 660 (m). UV–Vis (DMSO): 278 nm (ε = 22,822 M^{-1} cm^{-1}), 330 nm (ε = 26,030 M^{-1} cm^{-1}); (Buffer): 236 nm (ε = 18,004 M^{-1} cm^{-1}), 295 nm (ε = 11,582 M^{-1} cm^{-1}), 368 nm (ε = 2410 M^{-1} cm^{-1}). LC–MS: m/z 522.98 $[Au(A^2)Cl_2]^+$.

*[Au(A^3)Cl]·Cl_2 (**3**)*

Similar procedure was followed using A^4 as ligand, resulted in light orange precipitate. Yield: 91%, m.p.: 277 °C, Anal. Calc. for $C_{17}H_{13}AuCl_3N_5O_2$ (622.64): C, 32.79; H, 2.10; N, 11.25%. Found: C, 32.67; H, 2.22; N, 11.10%. Λm (1×10^{-3} mol L^{-1} in DMF): 138 mho cm^2 $mole^{-1}$. ^{1}H NMR ($CDCl_3$-*d*, 400 MHz): δ (ppm) 12.08 (s, 2H, —NH), 8.55 (d, 4H, $H_{3,5,6',6''}$, J = 5.2), 8.48 (dd, 2H, $H_{3',3''}$, J = 2, J = 7.6), 8.36 (t, 1H, H_4, J = 6.4), 8.12 (dt, 2H, $H_{4',4''}$, J = 1.6, J = 8.8), 7.40 (t, 2H, $H_{5',5''}$, J = 6.4). ^{13}C NMR ($CDCl_3$-*d*, 100 MHz): δ (ppm) 171.25 (C_{CO}), 152.64 ($C_{4',4''}$), 152.12 (C_4), 149.60 ($C_{2,6}$), 139.33 ($C_{6',6''}$), 136.17 ($C_{2',2''}$), 131.89 ($C_{3,5}$), 129.43 ($C_{5',5''}$), 114.51 ($C_{3',3''}$). FT-IR (cm^{-1}): 3600 (w), 3080 (m), 1720 (s), 1680 (s), 1640 (s), 1550 (s), 1440 (s), 1340 (w), 1300 (m), 840 (m), 680 (m). UV–Vis (DMSO): 244 nm (ε = 22,453 M^{-1} cm^{-1}), 280 nm (ε = 18,460 M^{-1} cm^{-1}); (Buffer): 259 nm (ε = 25,475 M^{-1} cm^{-1}), 290 nm (ε = 25,700 M^{-1} cm^{-1}). LC–MS: m/z 551.03 $[Au(A^1)Cl]^{2+}$.

*[Au(A^4)Cl_2]·Cl (**4**)*

Similar procedure was followed using A^4 as ligand, resulted in yellow precipitate. Yield: 82%, m.p.: 243 °C, Anal. Calc. for $C_{11}H_9AuCl_3N_3O$ (502.53): C, 26.29; H, 1.81; N, 8.36%. Found: C, 26.14; H, 1.97; N, 8.51%. Λm (1×10^{-3} mol L^{-1} in DMF): 102 mho cm^2 $mole^{-1}$. ^{1}H NMR ($CDCl_3$-*d*, 400 MHz): δ (ppm) 10.57 (s, 1H, —NH), 8.66 (d, 1H, H_6, J = 4.4), 8.46 (d, 1H, H_3, J = 9.6), 8.41 (t, 1H, H_4, J = 4.4), 8.33 (d, 1H, $H_{6'}$, J = 9.6), 7.94 (t, 1H, H_5, J = 8), 7.80 (t, 1H, $H_{4'}$, J = 8), 7.52 (dt, 1H, $H_{5'}$, J = 1.6, J = 4.8), 7.12 (dd, 1H, $H_{3'}$, J = 6.0, J = 10.8). ^{13}C NMR ($CDCl_3$-*d*, 100 MHz): δ (ppm) 168.34 (C_{CO}), 153.60 ($C_{4'}$), 152.05 (C_4), 149.89 (C_2), 144.61 (C_6), 137.42 ($C_{6'}$), 134.59 ($C_{2'}$), 132.94 (C_5), 130.70 ($C_{5'}$), 128.28 (C_3), 115.77 ($C_{3'}$). FT-IR (cm^{-1}): 3600 (m), 3090 (w), 1690 (s), 1670 (s), 1610 (s), 1570 (s), 1440 (s), 1340 (m), 1290 (m), 840 (s), 810 (s). UV–Vis (DMSO): 246 nm (ε = 11,740 M^{-1} cm^{-1}), 295 nm (ε = 8930 M^{-1} cm^{-1}); (Buffer): 231 nm (ε = 28,400 M^{-1} cm^{-1}), 285 nm (ε = 22,761 M^{-1} cm^{-1}), 315 nm (ε = 6028 M^{-1} cm^{-1}). LC–MS: m/z 465.97 $[Au(A^2)Cl_2]^+$.

*[Au(A^5)Cl_2]·Cl (**5**)*

Similar procedure was followed using A^5 as ligand, resulted in dark orange precipitate. Yield: 84%, m.p.: 238 °C, Anal. Calc. for $C_{12}H_{11}AuCl_4N_2$ (522.01): C, 27.61; H, 2.12; N, 5.37. Found: C, 27.77; H, 1.99; N, 5.59%. Λm (1×10^{-3} mol L^{-1} in DMF): 97 mho cm^2 $mole^{-1}$. ^{1}H NMR ($CDCl_3$-*d*, 400 MHz): δ (ppm) 8.76 (d, 1H, H_6, J = 5.6), 7.87 (t, 1H, H_4, J = 1.6), 8.62 (d, 1H, H_3, J = 8.0), 7.48 (t, 1H, H_5, J = 4.8), 7.35 (dd, 2H, $H_{3',5'}$, J = 4.0, J = 12), 6.84 (dd, 2H, $H_{2',6'}$, J = 4.0, J = 12), 6.17 (s, 1H, —NH), 4.78 (d, 2H, —CH_2, J = 4.4). ^{13}C NMR ($CDCl_3$-*d*, 100 MHz): δ (ppm) 154.30 (C_2), 149.76 (C_4), 144.48 (C_6), 139.88 ($C_{1'}$), 135.97 ($C_{4'}$), 129.76 ($C_{3',5'}$), 126.82 (C_3), 126.05 (C_5), 124.53 ($C_{2',6'}$), 47.63 (C_{CH}). FT-IR (cm^{-1}): 3410 (m), 3020 (m), 1670 (s), 1530 (s), 1470 (m), 1370 (w), 1320 (m), 1280 (s), 1190 (m), 800 (s), 730 (w). UV–Vis (DMSO): 277 nm (ε = 18,046 M^{-1} cm^{-1}); (Buffer): 288 nm (ε = 24,565 M^{-1} cm^{-1}), 319 nm (ε = 8032 M^{-1} cm^{-1}). LC–MS: m/z 484.97 $[Au(A^3)Cl_2]^+$.

Solution study

All complexes show very low solubility in water and in aqueous buffered solutions. The studies required dissolving the complexes in a small amount of DMSO followed by dilution with a large excess of buffer. So we recorded UV–Vis absorption spectra of the solution of gold(III) compounds in DMSO and by adding small amounts of freshly prepared, concentrated solutions of **1**–**2** in dimethyl sulfoxide (DMSO) to the reference buffer (10 mM

phosphate, pH 7.4). Electronic spectra of the resulting mixtures were monitored at 24 h.

Brine shrimp lethality bioassay

Brine shrimp lethality bioassay is widely used in the cytotoxic bioassay for the bioactive compounds. The brine shrimp, *Artemia cysts*, was used as a convenient monitor for the screening. The eggs of the brine shrimp were collected and hatched in artificial seawater for 48 h to mature shrimp called nauplii. The cytotoxicity assay was performed on brine shrimp nauplii using Meyer method. The test samples were prepared by dissolving in DMSO (not more than 50 μL in 2.5 mL solution) and sea water. A vial containing 50 μL DMSO diluted to 2.5 mL was used as a control. Then nauplii were applied to each of all experimental vials and control vial. After 24 h, the vials were inspected using a magnifying glass and the number of surviving nauplii in each vial were counted. The lethal concentrations of compounds resulting in 50% mortality of the brine shrimp (LC_{50}) from the 24 h counts and the dose–response data were transformed into a straight line by means of a trend line fit linear regression analysis (MS Excel version 7); the LC_{50} was derived from the best-fit line obtained.

Interaction between complexes and DNA

Binding of complex with Herring Sperm DNA

The binding behavior of the Au(III) complexes toward Herring Sperm DNA was assessed by monitoring the transformation in the absorptive nature of complex (66 μM) brought by varying the concentration of DNA by maintaining the [DNA]/[Complex] in the range of 0.05–0.25, effect of increasing amount of DNA was nullified by adding same aliquots of DNA to reference cell. Absorption data were utilized to calculate intrinsic binding constant (K_b) for the complexes using following equation,

$$[DNA]/(\varepsilon_a - \varepsilon_f) = [DNA]/(\varepsilon_b - \varepsilon_f) + 1/K_b(\varepsilon_b - \varepsilon_f) \quad (1)$$

ε_a, ε_f and ε_b corresponds to A_{obsd}/[Complex], the extinction coefficient for free complex and the extinction coefficient for the complexes in the fully bound form, respectively. [DNA] is the concentration of DNA in terms of base pairs. A plot of [DNA]/($\varepsilon_a - \varepsilon_f$) versus [DNA] gives K_b as the ratio of slope to the intercept [17].

Thermal DNA denaturation study

DNA melting experiments were carried out by monitoring the absorption intensity of Herring Sperm DNA (100 μM) at 260 nm in the range of 25 °C to 100 °C at increments of 0.5 °C min^{-1}, both in the absence and presence of the complexes. The melting temperature (T_m) of DNA was determined as the midpoint of the optically detected transition curves. The ΔT_m value was defined as the difference between T_m of the free DNA and T_m of the bound DNA.

Viscosity measurements

An Ubbelohde viscometer maintained at a constant temperature of 27 ± 0.01 °C in a thermostatic jacket, was used to measure the flow time of DNA in phosphate buffer (Na_2HPO_4/NaH_2PO_4, pH 7.2) with accuracy of 0.01 s. and precision of 0.1 s. DNA sample used was having approximate average length of 200 base pairs prepared by sonication to minimize the complexities arising from its flexibility [18]. Flow time for each sample was measured in triplicate and an average flow time was calculated. To evaluate the molecular extension from the intrinsic viscosity, [η], we used an equation'

$$[\eta] = (\pi N_A L^3/90 \times 10^3 Z)[3/(\ln 2p - 1.5) + 1/(\ln 2p - 2.5)] \quad (2)$$

where Z is the number of nucleotides per macromolecule. The expression in square brackets is rather insensitive to variations in p, for large p, and will be designated by $f(p)$. We are interested in the ratios $[\eta]/[\eta]_0$; from these we derive,

$$L/L_o = (\eta p_0/\eta_0 p)^{1/3} \quad (3)$$

where p is the axial ratio of the rods and subscript '0' indicate absence of complex. Since the hydrodynamic length of DNA molecule L/L_o, is directly proportional to the binding ratio of the complex to DNA, the cubic root of relative viscosity is proportional to the binding ratio of the complex to DNA. Representation of data was done in terms of $(\eta/\eta_0)^{1/3}$ versus concentration ratio ([Complex]/[DNA] = 0.04–0.2), where η is the viscosity of DNA solution in the presence of complex and η_0 is the viscosity of solution of DNA alone. Viscosity values were calculated using following equation, $\eta \propto (t - t_0)$; where t_0 is the flow time of buffer alone and t is the flow time for buffer containing DNA.

Gel electrophoresis

Electrophoresis through agarose is the standard method used to separate, identify, or purify DNA fragments. When an electric field is applied across the gel, DNA, which is negatively charged at neutral pH, migrates toward the anode. The intact supercoiled (SC, form I) DNA migrates faster than the single-nicked (OC, form II) DNA in the gel. The linear (L. Form III) DNA have an intermediate mobility. This technique has been employed to identify the products of DNA cleavage, which was carried out in this work.

Cleavage of pUC19 DNA (50 μM) by complexes (200 μM) was measured by the conversion of supercoiled pUC19 DNA to open vcircular (OC) and linear (L). Gel electrophoresis of pUC19 DNA was carried out in TAE buffer (0.04 M Tris–Acetate, pH 8.2, 0.001 M EDTA). 15 μL of reaction mixture contains 100 μg/mL plasmid DNA, and complex. Reaction mixture was incubated at 37 °C. All reactions were quenched by addition of 3 μL loading buffer (0.25% bromophenol blue, 40% sucrose, 0.25% xylene cyanole, and 200 mM EDTA). The aliquots were loaded directly onto 1% agarose gel and electrophoresed at 50 V in 1X TAE buffer. Gel was stained with 0.5 μg/mL of EB, and was photographed on a UV illuminator. After electrophoresis, the proportion of DNA in each fraction was estimated quantitatively from the intensity of the bands using AlphaDigiDoc™ RT. Version V.4.0.0 PC–Image software.

Kinetic measurements using the gel electrophoresis technique

For kinetic measurements, DNA cleavage rates at various complex concentrations were measured in a TAE buffer (pH 8.2) at 37 °C for different intervals of time (50–350 min). The decrease in the intensities of form I with time were then plotted against complex concentrations, and were fitted well with a single-exponential decay curve (pseudo-first-order kinetics) by use of Eq. (4), where y_0 is the initial percentage of a form of DNA, y is the specific form of DNA at time t, K_{obs} is the hydrolysis rate or apparent rate constant, and V_{max} is the maximal reaction velocity. Careful optimization of electrophoretic and densitometric techniques led to pseudo-first-order kinetics and allowed the determination of Michaelis–Menten kinetic parameters.

$$y = (100 - y_0)[1 - \exp(-K'_{obs}t)] \quad (4)$$

K'_{obs} versus [Complex] (50–350 μM) was plotted and fit using Eq. (5), which allows the determination of both the rate constants and Michaelis–Menten – "type" kinetic values. Similar experiments with constant complex concentrations and varying DNA (20–80 μM) concentrations were performed, and the intensities were plotted against substrate concentrations by use of Eq. (6).

$$K_{obs}' = V_{max}'[catalyst]/(K_M + [catalyst]) \quad (5)$$

$$K_{obs}' = V_{max}'[substrate]/(K_M + [substrate]) \quad (6)$$

Result and discussion

Synthesis and characterization

The complexes $[Au(A^n)Cl_x]Cl_y$, have been isolated from the ethanolic solution containing chloroauricacid as the starting material. Washing with ether gave the product in sufficiently pure form to record NMR spectra. All the complexes were obtained in good yield and were characterized by elemental analysis, ^1H and ^{13}C NMR, UV–Vis, FT-IR and LC–MS spectroscopic techniques. Elemental analysis data are in good agreement with the proposed structure. The molar conductivity data reveal that the complex 3 is 1:2 electrolytes, while other complexes are 1:1 electrolyte. The structure of various ligands and their coordination site are detailed in the Scheme 1.

In IR specta, shifting of the band ν(N—H) from 3420 (A^1) to 3490 (complex 1) cm^{-1}; 3430 (A^2) to 3490 (complex 2) cm^{-1}; 3390 (A^3) to 3600 (complex 3) cm^{-1}; 3350 (A^4) to 3600 (complex 4) cm^{-1} and 3330 (A^5) to 3410 (complex 5) cm^{-1} withdraw the possibility of deprotonation of —NH group and suggest the N atom of —NH group as coordinating atom.

The shifting of ν(C═N) band from 1240 (A^3) to 1340 (complex 3) cm^{-1} suggest N atom of central pyridyl ring as a coordinating atom. The low ν(C═O) band shifting from 1710 (A^3) to 1720 (complex 3) cm^{-1} ruled out the possibility of participation of keto group in coordination in complex 3. The shifting of ν(C═N) band from 1220 (A^4) to 1340 (complex 4) cm^{-1} suggest N atom of pyridine ring attached with keto group as a coordinating atom in complex 4. The shifting of ν(C═N) band from 1280 (A^5) to 1320 (complex 5) cm^{-1} suggest N atom of pyridine ring as a coordinating atom in complex 5.

In ^1H NMR spectra of complexes, the shifting of —NH peak from 5.27 (A^1) to 6.20 (complex 1) ppm; 5.26 (A^2) to 6.09 (complex 2) ppm; 11.26 (A^3) to 12.08 (complex 3) ppm; 10.45 (A^4) to 10.57 (complex 4) ppm and 4.86 (A^5) to 6.17 (complex 5) ppm supports the IR data. The coordination of ligand results in shifting of other ^1H NMR peaks to the downfield region.

The LC–MS spectrum of complexes validates the structure of complex proposed by above analytical and spectroscopic techniques. The LC–MS spectra and fragments correspond to peaks in LC–MS spectra of complexes 1–5 are shown in Supply 1–10.

UV–Vis spectra

Au(III) with its d^8 electronic configuration forms a variety of square-planar complexes. The low energy LMCT transitions are quite important for study of Au(III) complexes. The MLCT transitions do not play any role owing to the lack of reducing properties of Au(III). The time dependent spectrophotometric analyses of ligand to metal charge transfer transitions clearly showed that these complexes demonstrated no observable change in their UV–Vis spectra in DMSO and in 10 mM phosphate buffer which demonstrate the stability of these complexes in physiological conditions. However, the spectra of the samples dissolved in the reference buffer are different than in DMSO at room temperature, implying rapid hydrolysis of the coordinated chlorides of complexes and conversion into their hydroxy form. Such hydrolysis phenomena for Au(III) complexes has been also reported by Messori et al. [19]. The hydrolyzed metal chromophore $[Au(A)(OH)_x]^+$ fragment was sufficiently stable for at least 24 h in 10 mM phosphate buffer (pH 7.4) (physiological conditions). The LMCT region of metal complexes with their extinction coefficient values are shown in the experimental part.

Cytotoxicity

Considering that a bioassay is the first step necessary for the drug discovery process, the complexes were screened for *in vitro* toxicity using the microwell assay. This method allows the use of smaller quantities pure compounds, and permits a larger number of samples and dilutions within a shorter time. Brine shrimp

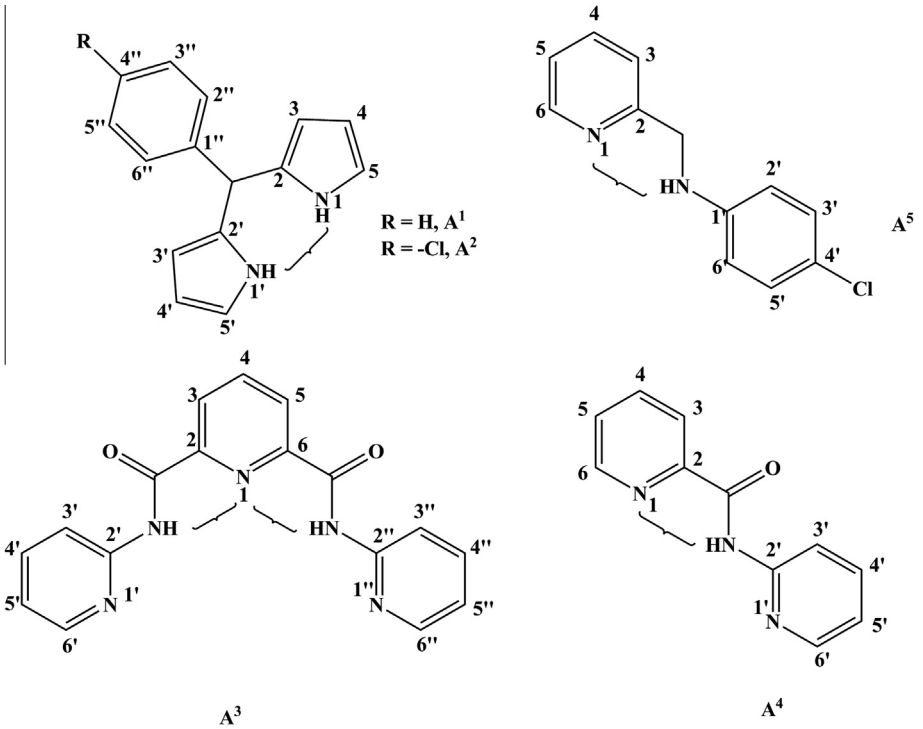

Scheme 1. Structure of the ligands.

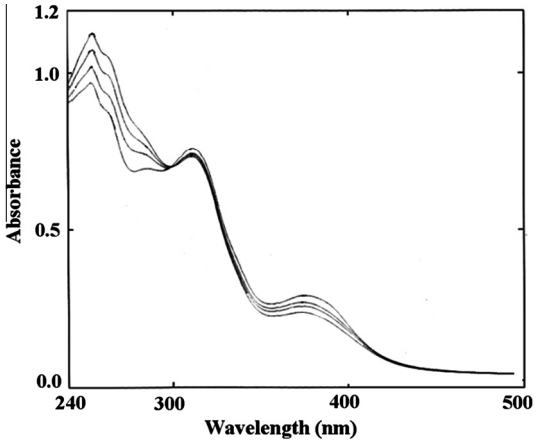

Fig. 1. Absorption spectral changes on addition of HS DNA to the solution of complex 1 after incubating it for 10 min at room temperature in phosphate buffer at 7.2 pH.

lethality bioassay is a recent development in the assay of bioactive compounds [20,21]. The LC_{50} (half-inhibition) values obtained after the analysis of complexes 1–5 are 10, 9, 20, 14 and 16 μM, respectively. The complexes may demonstrate cytotoxicity due to their ability to effectively interact with cellular DNA or the effect of the ligand on cellular uptake of the Au(III) complexes. Since the active species in the physiological conditions is $[Au(A)(OH)_x]^+$, we can assume that the mechanism of cytotoxic action of these agents is due to some combination of DNA interaction and redox activity of the Au(III) center. In attempt to better understand the role of each of these factors, DNA binding affinity studies for complexes have been carried out.

DNA binding study

UV–Vis absorption titration analysis

It is generally accepted that DNA is the primary target in the *cis*-platin mechanism [22]. Similarly, interactions between small molecules and DNA rank among the primary action mechanisms of cytotoxic activity. In order to compare the binding strength of the complexes with HS DNA, the intrinsic DNA binding constants (K_b) along with the binding site of the complexes to DNA are determined by monitoring the change of the absorption intensity of the charge transfer spectral band of the binary complexes with

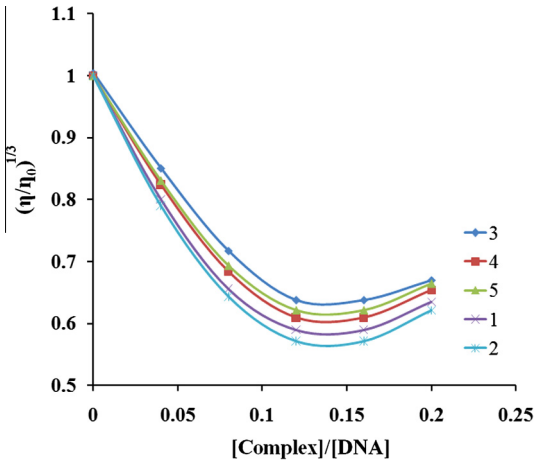

Fig. 2. Effect on relative viscosity of DNA under the influence of increasing amount of complexes at 27 ± 0.1 °C.

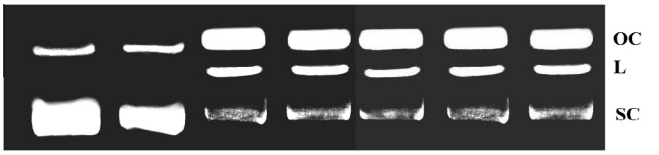

Fig. 3. Agarose gel (1%) of pUC19 (20 μM) at 37 °C in TE buffer (pH 8) with 150 μM complex 1–7. *Lane 1*, DNA control; *lanes 2*, DNA + metal salt; *lane 3*, DNA + complex 1; *lane 4*, DNA + complex 2; *lane 5*, DNA + complex 3; *lane 6*, DNA + complex 4; *lane 7*, DNA + complex 5.

increasing concentration of HS DNA. With increasing concentration of DNA added, significant hyperchromicity and red-shift was observed (Fig. 1). It suggests that complexes may covalently bind to DNA in the major or minor groove. Hyperchromism results from breakage of secondary structure of DNA due to the fact that phosphate group can provide the suitable anchors for coordination with complexes. The red shift indicates coordination of complex with DNA through N7 position of guanine. Such type of binding observed in many *cis*-platins, chloro-ruthenium and aqua-ruthenium complexes [23,24]. The binding constant (K_b) values for complexes 1–5 are 2.8×10^5, 2.9×10^5, 1.3×10^5, 2.3×10^5 and 2.1×10^5, respectively as calculated from Eq. (1).

Thermal DNA denaturation and viscosity measurement

Thermal behavior of DNA in the presence of metal complexes can give information about the interaction strength of the complexes with DNA. The double-stranded DNA tends to gradually dissociate to single strands on increase in the solution temperature and generates a hyperchromic effect on the absorption spectra of DNA bases (λ_{max} = 260 nm). In order to identify this transition process, the melting temperature T_m, which is defined as the temperature where half of the total base pairs gets non-bonded, is a valuable parameter. Strong interaction of compounds to DNA generally results in a considerable increase in the melting temperature (T_m). The DNA melting studies with the complexes 1–5 show a moderate positive shift in the melting temperature (ΔT_m) i.e. 6.2, 6.4, 5.2, 6.0 and 5.7 °C, respectively suggesting primarily intercalation or covalent binding nature.

To understand the nature of the interaction between the complexes and DNA, viscosity measurements were done. Viscosity parameter is important as it is sensitive to the change in length of the DNA strands and provides valuable information for any

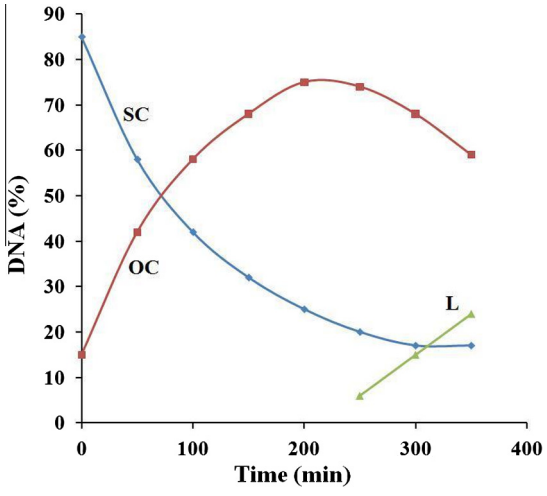

Fig. 4. Decrease in the SC form and formation of the OC and L form of pUC19 DNA in the presence of complex 1 (150 μM) with incubation time.

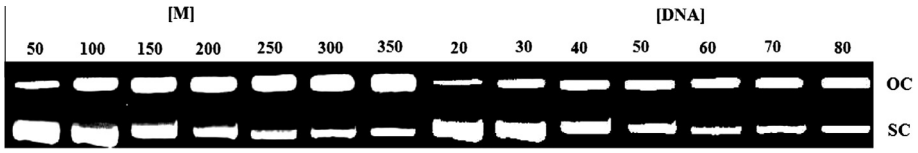

Fig. 5. Michaelis–Menten Reaction kinetics for the cleavage of plasmid DNA: *lane 1–7*, pseudo Michaelis–Menten kinetic, at constant DNA concentration ([substrate] = 50 μM) and varying complex 1 concentration ([catalyst] = 50–350 μM); *lane 8–14*, true Michaelic–Menten kinetic, at constant complex concentration ([catalyst] = 150) and varying DNA concentration ([substrate] = 20–80 μM).

conformational change [25]. Plot of relative specific viscosity $(\eta/\eta_0)^{1/3}$ versus [Complex]/[DNA] (Fig. 2) ratio shows decrease the relative viscosity of HS-DNA for all the complexes, consistent with partial intercalation or covalent nature of DNA binding, in which breakage or bending of DNA secondary structure is observed. This is accompanied by decrease in the relative viscosity due to shortening of length of the DNA chain. The results obtained from viscosity studies and thermal DNA denaturation studies as well as UV–Vis spectral titration validate the covalent binding nature of DNA interaction for all the complexes.

Nucleolytic activity on plasmid DNA

All the Au(III) complexes were subjected to series of time-dependent and concentration-dependent DNA cleavage experiments. All complex ions $[Au(A^n)(OH)_2]^+$ showed significant DNA cleavage properties due to their ability to interact with DNA, where the supercoiled DNA (form I) was cleaved to the relaxed open circular DNA (form II) over a period of 6 h as illustrated in Fig. 3. During this incubation period, complexes showed pronounced capability to further cleave form II to linear DNA (form III). The positive-charge on active chromophore group of complexes facilitate their interaction with negatively charged DNA and accelerate the cleavage of DNA, especially, complex 2 imparts higher cleavage activity on plasmid DNA than other complexes, consistent with other biological parameters.

Kinetic measurements for DNA cleavage by compounds

As a result of the very high efficiency of the complex ion $[Au(A^n)(OH)_2]^+$ in cleaving the strands of plasmid DNA, all complexes were subjected for detailed kinetics studies in order to explore their activities in the catalytic cleavage of plasmid DNA. The pUC19 DNA (50 μM) was incubated with complex (200 μM) in TE buffer at 37 °C for 50–350 min. The increase in the amount of OC and L forms of DNA was observed to be associated with the increase of reaction time (Fig. 4). The amount of linear DNA was 24%, 26%, 21%, 22%, and 24% when the reaction time was 350 min for complex 1–5, respectively. The decrease in the amount of SC form and the formation of OC form of DNA with time shows the exponential nature of the curves. The plot of ln(%SC DNA) versus time is linear, which confirms the process is pseudo-first-order. The rate constant k_1 (7.8×10^{-5}, 8.0×10^{-5}, 7.0×10^{-5}, 8.0×10^{-5} and 7.8×10^{-5} s^{-1} for complexes 1–5, respectively), the slope of the linear plot, was obtained using a complex concentration of 200 μM.

Plasmid DNA cleavage was monitored under 'pseudo' Michaelis–Menten kinetic conditions using a constant substrate DNA concentration (50 μM) and varying complex concentration (50–350 μM) (Fig. 5). The kinetic parameters for the pseudo-Michaelis–Menten conditions are derived from the plots of k_{obs} versus [catalyst] and fit to Eq. (5). Under these experimental conditions, values of K_M are 216, 231, 169, 208 and 193 μM for the complexes 1–5, respectively. These values represent pseudo-Michaelis–Menten conditions. The rate enhancements obtained here for complexes (2.8×10^7, 3.0×10^7 2.3×10^7, 2.8×10^7 and 2.8×10^7 for complexes 1–5, respectively) over the non-catalyzed DNA ($k = 3.6 \times 10^{-8}$ h^{-1} at 37 °C [26,27]) clearly reveals the efficiency of the complexes to cleave the double-stranded DNA.

Plasmid DNA cleavage was also monitored under 'true' Michaelis–Menten kinetic conditions using a constant complex concentration (150 μM) and varying substrate DNA concentration (20–80 μM) (Fig. 5). The cleavage rate constants, k_{obs} were estimated in a similar fashion as that shown by Eq. (4) and then plot of k_{obs} versus [substrate] was drawn. Under these experimental conditions, values of K_M are 76, 84, 68, 80 and 73 μM for complexes 1–5, respectively. The rate enhancements obtained here for complexes (2.2×10^7, 2.3×10^7, 1.8×10^7, 2.3×10^7 and 2.3×10^7 for complexes 1–5, respectively) over the non-catalyzed DNA reveals the efficiency of the complexes to cleave the double-stranded DNA.

Conclusion

The structural analysis that we have performed on mononuclear gold(III) complexes, relying on the availability of different spectroscopic data, has clearly revealed the existence of a common and well-conserved structural motif comprising the gold center, chloride atoms, and ligand within a square planar arrangement. Solution study indicates that ligand configuration appears to impart suitable stability of the hydroxy species under aqueous physiological condition. Also the hydroxy chromophore is stable for 24 h under the physiological condition. Then efforts were made to correlate the cytotoxic properties of the gold(III) complexes with their DNA interaction properties and notably, positive correlation has emerged. The complexes show potent cytotoxic properties against *Artemia cysts* and the possible observed covalent interaction of complexes with DNA at N7 position of guanine base could be the target. Furthermore, Michelis–Menten kinetic study on plasmid DNA, which shows rate enhancement ratio of the complexes in the order of 10^7 in cleaving DNA over non-catalyzed DNA, also supported above correlation data. Such correlations might be further exploited to design new and more-active gold-based anticancer agents and presents the attractive possibility of activating the cleavage chemistry of covalently bound complexes.

Acknowledgments

Authors thank Head, Department of Chemistry Sardar Patel University, India for making it convenient to work in laboratory and CSIR, India for providing financial support under "CSIR-Senior Research Fellowship" scheme.

Appendix A. Supplementary material

Supplementary data associated with this article can be found, in the online version, at http://dx.doi.org/10.1016/j.saa.2013.03.037.

References

[1] S.R. Grguric-Sipka, R.A. Vilaplana, J.M. Perez, M.A. Fuertes, C. Alonso, Y. Alvarez, T.J. Sabo, F. Gonzalez-Vilchez, J. Inorg. Biochem. 97 (2003) 215–220.
[2] S. Rauf, J.J. Gooding, K. Akhtar, M.A. Ghauri, M. Rahman, M.A. Anwar, A.M. Khalid, J. Pharm. Biomed. Anal. 37 (2005) 205–217.

[3] B. Rosenberg, L. Van Camp, J.E. Trosko, V.H. Mansour, Nature 222 (1969) 385–386.
[4] P.U. Maheswar, V. Rajendiran, M. Palaniandavar, R. Parthasarathi, V. Subramanian, J. Inorg. Biochem. 100 (2006) 3–17.
[5] P.B. Sreeja, M.R. Prathapachandra Kurup, A. Kishore, C. Jasmin, Polyhedron 23 (2004) 575–581.
[6] E. Kikuta, N. Katsube, E. Kimura, J. Biol. Inorg. Chem. 4 (1999) 431–440.
[7] M.A. Jakupec, M. Galanski, B.K. Keppler, Rev. Physiol. Biochem. Pharmacol. 146 (2003) 1–53.
[8] W.I. Sundquist, S.J. Lippard, Coord. Chem. Rev. 100 (1990) 293–322.
[9] T.W. Hambley, J. Chem. Soc. Dalton Trans. (2001) 2711–2718.
[10] T.A. van den Berg, B.L. Feringa, G. Roelfes, Chem. Commun. (2007) 180–182.
[11] P.J. Sadler, M. Nasar, V.L. Narayanan, Platinum Coordination Complexes in Cancer Chemotherapy, Martinus Nijhoff, Boston, 1984.
[12] I. Ott, Coord. Chem. Rev. 253 (2009) 1670–1681.
[13] V. Gandin, A.P. Fernandes, M.P. Rigobello, B. Dani, F. Sorrentino, F. Tisato, M. Bornstedt, A. Bindoli, A. Sturaro, R. Rella, C. Marzano, Biochem. Pharmacol. 79 (2010) 90–101.
[14] M.N. Patel, B.S. Bhatt, P.A. Dosi, Appl. Biochem. Biotech. 166 (2012) 1949–1968.
[15] C.H. Lee, J.S. Lindsey, Tetrahedron 50 (1994) 11427–11440.
[16] B.J. Littler, M.A. Miller, C.H. Hung, R.W. Wagner, D.F. O'Shea, P.D. Boyle, J.S. Lindsey, J. Org. Chem. 64 (1999) 1391–1396.
[17] A. Wolfe, G.H. Shimer, T. Meehan, Biochemistry 26 (1987) 6392–6396.
[18] G. Cohen, H. Eisesberg, Biopolymers 8 (1969) 45–55.
[19] L. Messori, P. Orioli, C. Tempi, G. Marcon, Biochem. Biophys. Res. Commun. 281 (2001) 352–360.
[20] B.N. Meyer, N.R. Ferrigni, J.E. Putnam, J.B. Jacobsen, D.E. Nicholsand, J.L. Mclaughlin, Planta Med. 45 (1982) 31–34.
[21] B. Ahmad, S. Azam, S. Bashir, F. Hussain, M.I. Chaudhary, African J. Biotech. 10 (2011) 1448–1453.
[22] C.X. Zhang, S.J. Lippard, Curr. Opin. Chem. Biol. 7 (2003) 481–489.
[23] M. Chauhan, F. Arjmand, J. Organomet. Chem. 692 (2007) 5156–5164.
[24] N. Grover, T.W. Welch, T.A. Fairley, M. Cory, H.H. Thorp, Inorg. Chem. 33 (1994) 3544–3548.
[25] P.R. Chetana, R. Rao, M. Roy, A.K. Patra, Inorg. Chim. Acta 362 (2009) 4692–4698.
[26] A. Barve, A. Kumbhar, M. Bhat, B. Joshi, R. Butcher, U. Sonawane, R. Joshi, Inorg. Chem. 48 (2009) 9120–9132.
[27] A. Sreedhara, J.D. Freed, J.A. Cowan, J. Am. Chem. Soc. 122 (2000) 8814–8824.